JAM CM Journal of Applied Mathematics and Computational Mechanics 2020, 19(2), 59-71
www.amcm.pcz.pl p-ISSN 2299-9965
DOI: 10.17512/jamcm.2020.2.05 e-ISSN 2353-0588

TWO DIMENSIONAL ANISOTROPIC MACROSCOPIC SECOND-ORDER TRAFFIC FLOW MODEL

Gabriel Obed Fosu[1], Francis Tabi Oduro[2]

[1] *Department of Mathematics, Presbyterian University College, Ghana*
[2] *African Institute for Mathematical Sciences, Ghana*
gabriel.obed@presbyuniversity.edu.gh, francis@aims.edu.gh

Received: 25 September 2019; Accepted: 9 April 2020

Abstract. In the past, the density-gradient term of second-order macroscopic models was replaced with a speed-gradient term to rectify the rearward movement of traffic waves. Hither, a classical speed-gradient macroscopic model is extended to account for the lateral flow dynamics on a multi-lane road. The anisotropic model is modified to capture some inherent vehicular multi-lane traffic features; lateral viscosity and velocity differentials. These variables are quantized within the scope of a two-dimensional spatial domain as opposed to the existing one-dimensional model. A detailed exemplification of acceleration and deceleration waves, stop-and-go waves, and cluster effects are presented to explain the path of information flow. All these non-linear flow properties are evident throughout the simulation.

MSC 2010: *35L40, 76M20,35Q30, 76L05*
Keywords: *viscosity, macroscopic model, traffic waves, Jiang-Wu-Zhu model, cluster effects*

1. Introduction

The traffic flow equation by Lighthill and Whitham [1], together with Richards [2], is one of the most widely used models for traffic analysis. It is simply called the LWR model. It is described by a single equation following a similar principle as the continuity equation. However, the LWR model was criticized based on the following. The inability of the model to describe traffic breakdown. LWR models have infinite acceleration. Traffic capacity and the characteristic waves are determined entirely by the finite speed adaptation times and reaction times. There is the absence of inertial effect in the LWR model, hence an instantaneous adjustment of vehicle velocity. Drivers are not able to predict in advance the changes in traffic conditions, thus the difficulty adjusting their speed to the average velocity [3–5].

Due to these flaws, the dynamic velocity equation was developed along with the LWR to model these shortcomings. This speed equation originated from the writings of Payne [3] and Whitham [6]. Later, the second-order isotropic equation was again flawed for its backward traveling wave properties [7]. This led to the development of

models having anisotropic property. The most common among these are the Zhang models [8, 9], Aw-Rascle Model [10], and the Jiang-Wu-Zhu (JWZ) model [11]. Zhang proposed a non-equilibrium model devoid of gas-like behavior. Aw and Rascle replaced the space derivative with a convective derivative. Jiang, Wu, and Zhu replaced the density gradient component in the Payne-Whitham model with a speed gradient quantity. These authors made these modifications to resolve the backward traveling wave critic by Daganzo. In the recent past, anisotropic and isotropic models have been extended to address more realistic traffic phenomenon. The Payne-Whitham model has been extended to capture driver physiological response [12] and driver reaction to traffic stimuli [13]. The Jiang-Wu-Zhu has been extended to account for diffusion [14], whereas the Zhang and Aw-Rascle models have been extended to explicitly model lane-changing behavior on motorways [15].

However, these second-order models have not explicitly accounted for viscosity for multi-lane traffic flow. An earlier attempt to model resistance was through the diffusion models [16–18]. These models were presented within a one-dimensional spatial domain as opposed to viscosity that is observable within a two-dimensional spatial domain. In this paper, we present a two-dimensional macroscopic model that accounts for viscosity. An additional source term is introduced into the dynamics velocity equation to model traffic viscosity. This new quantity is derived from the theory of fluid dynamics and illustrated through the physics of non-slip condition in Figure 1.

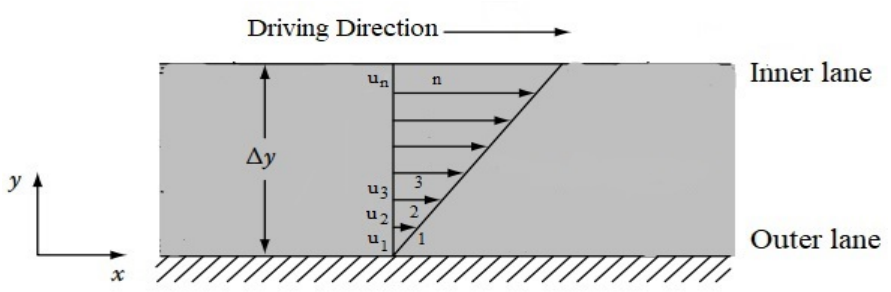

Fig. 1. Velocity differentials across fluid flow [19]

This figure is loosely used to illustrate an arbitrary multi-lane flow. It is assumed that the velocities of this flow differ from lane to lane. The velocities for lanes $1, 2, \cdots, n$ are $u_1, u_2, \cdots, u_n$ respectively. The speed increases by moving towards the inner lanes. Vehicles on lane n have the greater speed, whereas vehicles on lane *1* have the least speed. With this characterization, the inter-lane traffic resistance can be modeled using Newton's law of viscosity

$$\rho = \vartheta * du/dy \tag{1}$$

ρ is used to denote the total shear effect. ϑ is the viscosity rate. This explains the resistance of the traffic to shear forces. The rate is smaller when two adjacent vehicles

have little impact on each other. The speed differential du/dy accounts for the speed changes of adjacent vehicles driving in the same direction at a given point in time. For instance, if vehicle A is speeding at $\Phi_1 m/s$ on lane m at time t, and vehicle B has speed $\Phi_2 m/s$ on lane $m+1$ at the same time and location, then the velocity gradient $du/dy = |\Phi_1 m/s - \Phi_2 m/s|$. Thence, the researchers seek to incorporate the term $\vartheta * du/dy$ into the existing class of macroscopic models.

The following sections are organized as follows: In section 2, a new dynamic velocity equation is derived from a reduced Navier-Stokes equation. The properties of this viscous model are presented in section 3. It is followed by a numerical solution of this system of equations. The solution characterizes some nonlinear dynamic traffic properties such as shock-wave and rarefaction wave effects, stop-and-go traffic, and local cluster effects. In section 6, we present a general summary of the entire paper.

2. The model derivation

Second-order macroscopic traffic flow models are constituted by two equations; the LWR equation and an acceleration equation. The LWR model is expressed as

$$\frac{\partial k(x,t)}{\partial t} + \frac{\partial q(x,t)}{\partial x} = 0 \tag{2}$$

where $k(x,t)$ is the density, $u(x,t)$ is the speed and $q(x,t) = k(x,t)u(x,t)$ is the flow rate.

As stated afore, the acceleration equation was introduced to overcome the shortcomings of the LWR model. In this section, we derive a new dynamic velocity equation from the reduced Navier-Stokes equation. From [20], the two-dimensional Navier-Stokes equation is expressed as:

$$k\left(\frac{\partial u}{\partial t} + u\frac{\partial u}{\partial x} + v\frac{\partial u}{\partial y}\right) = g_x - \frac{\partial P}{\partial x} + \vartheta\left(\frac{\partial^2 u}{\partial^2 x} + \frac{\partial^2 u}{\partial^2 y}\right) \tag{3a}$$

$$k\left(\frac{\partial v}{\partial t} + u\frac{\partial v}{\partial x} + v\frac{\partial v}{\partial y}\right) = g_y - \frac{\partial P}{\partial y} + \vartheta\left(\frac{\partial^2 v}{\partial^2 x} + \frac{\partial^2 v}{\partial^2 y}\right) \tag{3b}$$

ϑ is the viscosity rate, P is the pressure, g_x and g_y are the gravitational forces, respectively, k is the density, u is the speed in the x-direction and v is the speed in the y-direction. From the physics of traffic flow (Fig. 1), we realize that there is zero flow in the y-direction; hence v and its derivative go to zero. Thus, (3b) ceases to exist and equation (3) reduces to

$$k\left(\frac{\partial u}{\partial t} + u\frac{\partial u}{\partial x}\right) = g_x - \frac{\partial P}{\partial x} + \vartheta\left(\frac{\partial^2 u}{\partial^2 x} + \frac{\partial^2 u}{\partial^2 y}\right) \tag{4}$$

In deriving the lateral velocity gradient term, the quantity $\partial^2 u/\partial^2 y$ is decoupled as a constant and a first derivative term

$$\frac{\partial^2 u}{\partial y^2} \approx f_y \frac{\partial u}{\partial y}$$

The quantity f_y is used to delineate traffic sensitivity. This parameter will be modeled in parallelism to the sensitivity term in microscopic models [21, 22]. Note that the diffusive term is assumed to be zero. As the inter-lane gap between two adjoining vehicles declines, their velocities reduce as well. In other words, the flux reduces as traffic becomes viscous. In accounting for this, a negative sign is introduced to capture this relationship

$$k\left(\frac{\partial u}{\partial t} + u\frac{\partial u}{\partial x}\right) = g_x - \frac{\partial P}{\partial x} - \vartheta\left(f_y \frac{\partial u}{\partial y}\right) \tag{5}$$

Continuing from (5), the net impact of pressure force is replaced with the relaxation term $[V(k)-u]/\tau$ from the classical JWZ model. This is introduced to ensure that vehicles do not collide with each other. Another important term in the classical equation is the speed gradient. The authors brought in the gradient term $c_1 * \partial u/\partial x$ to address the problem of backward reaction to stimuli by drivers. c_1 is the driver anticipation rate. This quantity is directly imported from the classical model into this new formulation. Finally, g_x is assumed to be zero. Therefore, the new dynamic velocity equation is expressed as:

$$\frac{\partial u(x,t)}{\partial t} + u(x,t)\frac{\partial u(x,t)}{\partial x} = \frac{V(k(x,t)) - u(x,t)}{\tau} + c_1 \frac{\partial u(x,t)}{\partial x} - \vartheta \frac{f_y}{k(x,t)} \frac{\partial u(x,t)}{\partial y} \tag{6}$$

This new dynamic velocity equation (6) coupled with the LWR model (2) form the two-dimensional viscous anisotropic second-order macroscopic traffic flow model.

3. Properties of the viscous macroscopic model

The two-dimensional model is given as

$$\frac{\partial k(x,t)}{\partial t} + \frac{\partial q(x,t)}{\partial x} = 0 \tag{7a}$$

$$\frac{\partial u(x,t)}{\partial t} + u(x,t)\frac{\partial u(x,t)}{\partial x} = \frac{V(k(x,t)) - u(x,t)}{\tau} + c_1 \frac{\partial u(x,t)}{\partial x} - \vartheta \frac{f_y}{k(x,t)} \frac{\partial u(x,t)}{\partial y} \tag{7b}$$

Equation (7) is expressed in its quasi-linear form as:

$$\frac{\partial}{\partial t}\begin{bmatrix} k(x,t) \\ u(x,t) \end{bmatrix} + \begin{bmatrix} u(x,t) & k(x,t) \\ 0 & u(x,t) - c_1 \end{bmatrix} \frac{\partial}{\partial x}\begin{bmatrix} k(x,t) \\ u(x,t) \end{bmatrix} = \begin{bmatrix} 0 \\ \dfrac{V(k(x,t)) - u(x,t)}{\tau} - \vartheta \dfrac{f_y}{k(x,t)} \dfrac{\partial u(x,t)}{\partial y} \end{bmatrix} \tag{8}$$

let $\Psi = \begin{bmatrix} k(x,t) \\ u(x,t) \end{bmatrix}$, $C(\Psi) = \begin{bmatrix} u(x,t) & k(x,t) \\ 0 & u(x,t)-c_1 \end{bmatrix}$

and $D(\Psi) = \begin{bmatrix} 0 \\ \dfrac{V(k(x,t))-u(x,t)}{\tau} - \vartheta \dfrac{f_y}{k(x,t)} \dfrac{\partial u(x,t)}{\partial y} \end{bmatrix}$, then equation (8) becomes

$$\frac{\partial \Psi}{\partial t} + C(\Psi)\frac{\partial \Psi}{\partial x} = D(\Psi) \tag{9}$$

The characteristic variables of the homogeneous model are obtained by first computing for the eigenvalues of the matrix $C(\Psi)$. The eigenvalues are computed as follows

$$\begin{bmatrix} u(x,t)-\lambda & k(x,t) \\ 0 & u(x,t)-c_1-\lambda \end{bmatrix} = 0$$

$$[u(x,t)-\lambda][u(x,t)-c_1-\lambda] = 0 \quad \text{and} \quad \lambda_1 = u(x,t)-c_1, \quad \lambda_2 = u(x,t)$$

Since the parameter c_1 is assumed to be greater than zero, the viscous model is strictly hyperbolic. These eigenvalues commensurate that driver behavior is not affected by backward stimuli. The speed of the traffic exceeds the characteristic wave speeds, thus, the anisotropic phenomenon of traffic flow is conserved.

In order to compute for the eigenvectors, we use the expression

$$\begin{bmatrix} u(x,t)-[u(x,t)-c_1] & k(x,t) \\ 0 & u(x,t)-c_1-u(x,t)+c_1 \end{bmatrix} \begin{bmatrix} x_1 \\ x_2 \end{bmatrix} = 0$$

Therefore, the matrix of eigenvectors is also computed as:

$$M = \begin{bmatrix} -\dfrac{k(x,t)}{c_1} & 1 \\ 1 & 0 \end{bmatrix} \quad \text{with the inverse} \quad M^{-1} = \begin{bmatrix} 0 & 1 \\ 1 & \dfrac{k(x,t)}{c_1} \end{bmatrix} \tag{10}$$

The matrix of eigenvectors and its inverse are used to compute for the compatibility equations. Multiplying equation (9) by M^{-1}, we have

$$M^{-1}\frac{\partial \Psi}{\partial t} + M^{-1}C(\Psi)\frac{\partial \Psi}{\partial x} = M^{-1}D(\Psi) \tag{11}$$

Considering any small change in $\delta\Psi$, then the Riemann variables $r_{1,2}$ are deduced as

$$\delta r = M^{-1}\delta\Psi \qquad \text{and inversely as} \qquad \delta\Psi = M\delta r \tag{12}$$

That is to say that

$$\frac{\partial \Psi}{\partial t} = M\frac{\partial r}{\partial t} \qquad \text{and} \qquad \frac{\partial \Psi}{\partial x} = M\frac{\partial r}{\partial x} \tag{13}$$

Substituting equation (13) into (11), we obtain

$$M^{-1}M\frac{\partial r}{\partial t}+M^{-1}C(\Psi)M\frac{\partial r}{\partial x}=M^{-1}D(\Psi)$$

as required.

From equation (12), $\delta r = M^{-1}\delta\Psi$ can be recast as:

$$\delta\begin{bmatrix}r_1\\r_2\end{bmatrix}=\begin{bmatrix}0 & 1\\1 & \dfrac{k(x,t)}{c_1}\end{bmatrix}\delta\begin{bmatrix}k(x,t)\\u(x,t)\end{bmatrix}$$

with

$$\delta r_1=\delta u(x,t) \quad \text{and} \quad \delta r_2=\delta k(x,t)+\frac{k(x,t)}{c_1}\delta u(x,t) \tag{14}$$

By integrating both sides of (14), we obtain the wave propagation paths for the viscous JWZ model as

$$r_1=u(x,t) \quad \text{and} \quad r_2=k(x,t)+\frac{1}{c_1}u(x,t)$$

The propagation of r_1 is along the characteristic $u(x,t)$, whereas the propagation of r_2 is along the characteristic $u(x,t)-c_1$. The characteristic speed $u(x,t)-c_1$ is associated with a shock-wave and a rarefaction wave. These are illustrated graphically in the next section. The eigenvalue $u(x,t)$ linearly degenerate.

4. Numerical solution of the viscous macroscopic model

The first upwind finite difference scheme is used to solve the viscous JWZ model [11, 14]. The modified model is solved as a Riemann problem using the following initial condition:

$$k(x,0)=\begin{cases}k_l(x,t), & \text{if } x>mid_x\\k_r(x,t), & \text{if } x\le mid_x\end{cases} \quad \text{and} \quad u(x,0)=\begin{cases}u_l(x,t), & \text{if } x>mid_x\\u_r(x,t), & \text{if } x\le mid_x\end{cases}$$

where $k_l(x,t)$ and $u_l(x,t)$ are the upstream density and speed respectively. $k_r(x,t)$ and $u_r(x,t)$ are the downstream commensurate terms. mid_x divides the assumed road section into two halves. The formation and dissolution of queues from a given point (e.g. traffic light) is explored using these initial conditions. $k_l(x,t)$ less than $k_r(x,t)$ signifies a platoon of high speed vehicles reaching up with a platoon of slower vehicles or stopped vehicles. The opposite $k_l(x,t)$ greater than $k_r(x,t)$ shows the dissolution of a traffic jam.

The discrete version of the viscous JWZ model is expressed by equations (15) and (16). For the first updating equation, the discretized form is given as

$$k(i,j+1) = k(i,j) + \frac{\Delta t}{\Delta x} u(i,j)\left[k(i-1,j) - k(i,j)\right] + \frac{\Delta t}{\Delta x} k(i,j)\left[u(i,j) - u(i+1,j)\right] \tag{15}$$

whereas the dynamic velocity equation is given as

$$\begin{aligned} u(i,j+1) = u(i,j) &+ \frac{\Delta t}{\Delta x}\left[c_1 - u(i,j)\right]\left[u(i,j) - u(i-1,j)\right] \\ &- \frac{\Delta t}{\Delta y}\frac{\vartheta f_y}{k(i,j)}\left(u_m(i,j) - u_{m+1}(i,j)\right) + \frac{\Delta t}{\tau}\left(V(i,j) - u(i,j)\right) \end{aligned} \tag{16}$$

The spatial step sizes are $i, m \in \mathbb{N}$. $j \in \mathbb{W}$ is the time discretization size. $V(i,j)$ is defined by the underlying fundamental equation [23]

$$V(i,j) = u_{max}\left\{1 - exp\left[1 - \exp\left(\frac{k_m}{u_{max}}\left(\frac{k_{max}}{k(i,j)}\right) - 1\right)\right]\right\} \tag{17}$$

k_m is the speed of the kinematic wave during congestion. Given the initial density and speed profiles, equations (15) and (16) are used to determine the density and speed profiles at the next time step $j+1$.

The Courant-Friedrichs-Lewy (CFL) is used to ascertain the condition for convergence of the numerical scheme [24]. The CFL is a necessary condition for the stability of the numerical method. Given this viscous model, the numerical scheme is stable if

$$\max\left\{u_{max} - c_1, q'(k(x,t))\right\} \cdot \frac{\Delta t}{\Delta x} \leq 1 \tag{18}$$

4.1. Simulation results

The following realistic values are adopted for the simulation. A hypothetical road length (L) of 20 kilometers is divided into 100 equally spaced sizes. The simulation will span 10 minutes, with a time interval of 1 s. The maximum density is standardized with k_{max} equal unity. The anticipation rate $c_1 = 11$ m/s = $= k_m, \vartheta = 0.011$, and $\tau = 10$ s [11]. Inter lane sensitivity $f_y = 0.37$ s^{-1} as deduced from [22]. The free-flow speed is 30 m/s. According to the international European report, the maximum speed limit for a motorway is 33.333 m/s, an express road is 27.778 m/s, and a normal road is 22.225 m/s [25]. Hence, the lateral velocity gradient is deduced as 5.55 m/s in absolute terms for driving on adjacent lanes.

We present two graphical illustrations for shock-wave traffic. The case when the traffic light turns red (Fig. 2), and a situation of a free-flow flowing traffic merging with somewhat dense traffic (Fig. 3). The instances when the traffic light turns green (Fig. 4), and slightly dense traffic catches up with a normal flow (Fig. 5) are the two exemplifications for rarefaction waves.

The graphical plot (Fig. 2) depicts heavy dense traffic upstream merging with a stopped queue. There is the formation of long queues with a jam density traveling backward. The maximum speed of vehicles reduces to 5 m/s.

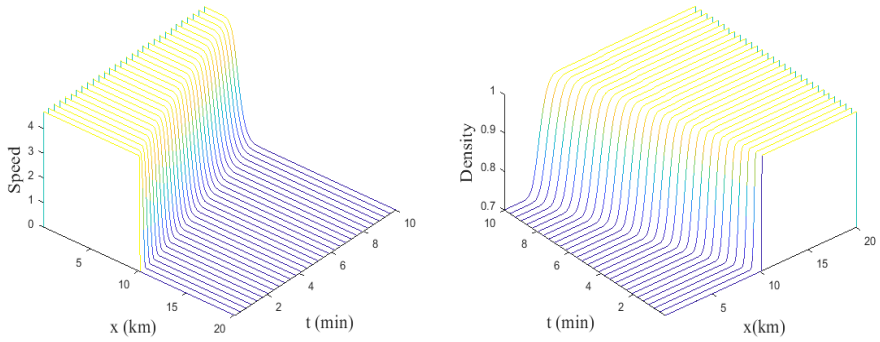

Fig. 2. Shock wave profiles with initial density $k_l = 0.7$ and $k_r = 1$

In Figure 3, both densities, up and down the discontinuity, are below the average concentration value. Nonetheless, the frontal density is greater. Hence, the traffic breakdown is not easily observable. Vehicles in the first half after the discontinuity can still achieve maximum speed. There is no stopped traffic within the first few minutes of the simulation, all the same, the queue begins to form after some time interval.

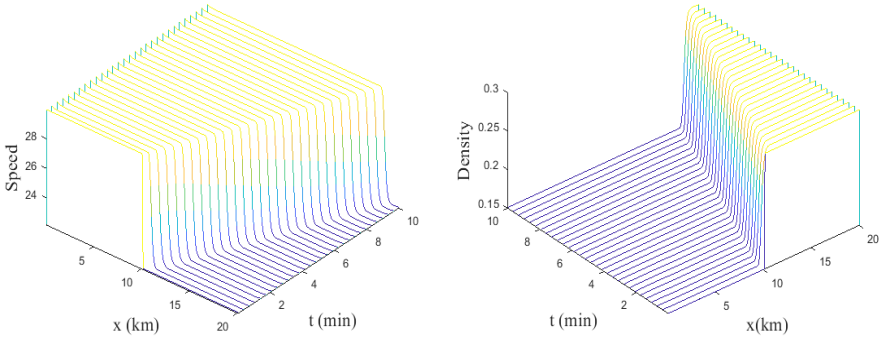

Fig. 3. Shock wave profiles with initial density $k_l = 0.15$ and $k_r = 0.3$

Figure 4 describes very dense traffic (almost coming to a complete stop) approaching a near-empty road. A likely related illustration is when the traffic turns green. The queue dissolves gradually with time. There is no stopped vehicle in the queue at the end of the simulation time.

From Figure 5, the densities upstream and downstream are above and below the average density respectively. Noticeably, the traffic dissolves moderately with time. There is neither a jam density nor a zero density. The flow of vehicles continues at an average, uninterrupted speed.

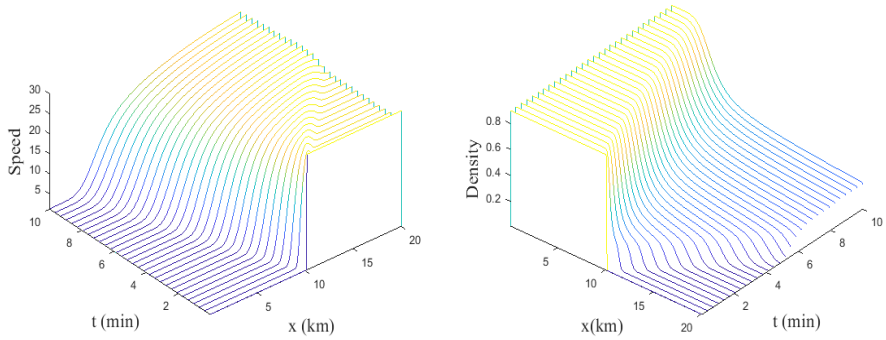

Fig. 4. Rarefaction wave profiles with initial density $k_l = 0.9$ and $k_r = 0.01$

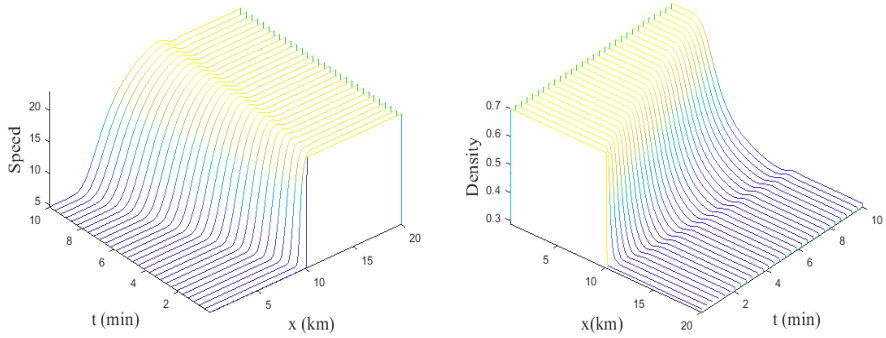

Fig. 5. Rarefaction wave profiles with initial density $k_l = 0.7$ and $k_r = 0.3$

These results demonstrate a realistic highway traffic phenomenon. The model can explicate a platoon of high-speed traffic conceding with either jammed traffic or fairly jammed traffic. The reverse, a platoon of jam traffic conceding with high-speed vehicles is also revealed through these analyses.

A further simulation is carried out to determine how the rate of viscosity influences the speed of vehicles. Different viscous rates are selected by the researchers to explore its role in traffic analysis. From Figure 5, vehicles leaving the jam could attain the maximum speed with ϑ equal 0.011. With similar illustrations in Figure 6, the speed of the vehicles decreases as ϑ is made to increase. Generally, it can be observed that rates greater than 0.011 have tendencies to disrupt the flow of traffic and eventually cause the traffic to come to a stop. Note that this speed drop is not as a result of a surge in density, rather, it is attributed to a lateral traffic impediment. This illustration indicates that viscosity is an important element in macroscopic traffic modeling.

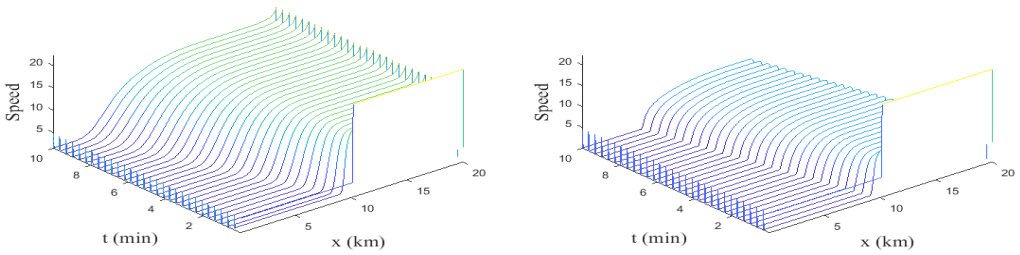

(a) $\vartheta = 0.11$ (b) $\vartheta = 0.21$

(c) $\vartheta = 0.31$ (d) $\vartheta = 1.11$

Fig. 6. Dissolution of traffic for different values of ϑ with the initial density $k_l = 0.7$ and $k_r = 0.3$

5. Cluster effects

A local perturbation of steady traffic may either blow-up or go into extinction. Homogeneous traffic will continue in its original state after some displacement when the prevailing density is way below/above the critical density. When the concentration is within certain neighborhood values of the critical density, an infinitesimal displacement will cause the traffic to blow-up over time. The amplification of this displacement through the traffic medium is referred to as local cluster effects or simply cluster effects [26].

Now, an inquiry is made to authenticate the model's strength in capturing this clustering process. A boundary condition of the form

$$k(L,t) = k(0,t), \qquad u(L,t) = u(0,t)$$

is employed for this interrogation. The following initial profile (19) and the fundamental equation (20) by [17] are adopted for this cluster analysis.

$$k(x,0) = k_o + \Delta k_o \left\{ \cosh^{-2}\left[\frac{160}{L}\left(x - \frac{5L}{16}\right)\right] - \frac{1}{4}\cosh^{-2}\left[\frac{40}{L}\left(x - \frac{11L}{32}\right)\right]\right\} \quad (19)$$

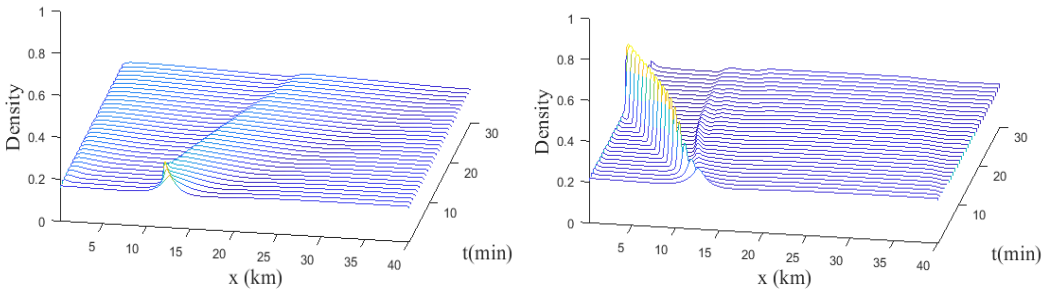

(a) $k_0 = 0.17$ (b) $k_0 = 0.22$

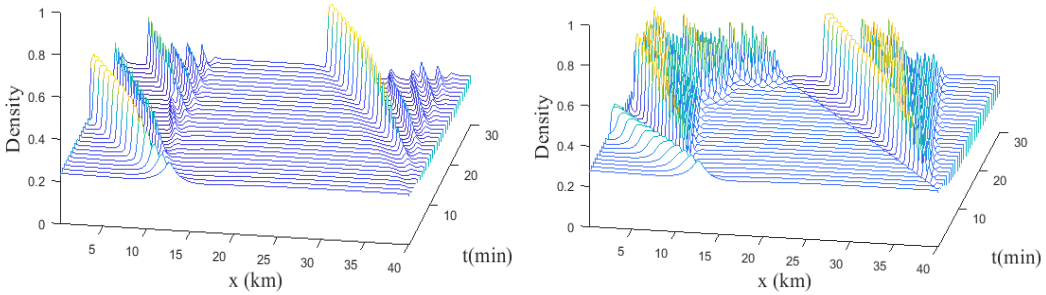

(c) $k_0 = 0.24$ (d) $k_0 = 0.28$

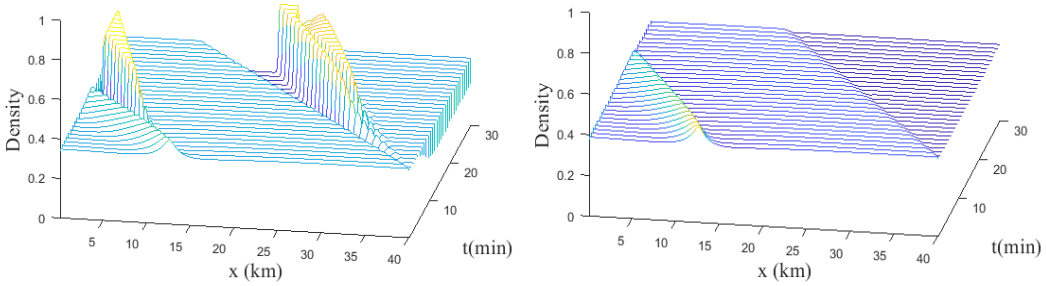

(e) $k_0 = 0.35$ (f) $k_0 = 0.39$

Fig. 7. Space-time evolution of density after some perturbations

The steady state speed density equation is given as:

$$V(k(x,t)) = u_{max}\left\{\left[1+\exp\left(\frac{k/k_{max}-0.25}{0.06}\right)\right]^{-1} - 0.00000372\right\} \qquad (20)$$

k_o is the initial constant density and $\Delta k_o = 0.1$ veh/m is the amplitude of a local disturbance. Except $L = 40$ km, all other parameters have the same connotation as in section 4. The initial density k_o will remain as a free parameter in order to quantize the range for this cluster effects.

From a zero reference point, this local effect is more evident by increasing the initial density. Then, beyond a certain threshold value, the effect begins to subside. We would observe a different cluster formation when the traffic concentration is between the values of 0.18 veh/m and 0.38 veh/m (Fig. 7b-7e). Outside this range of values, any amplification dies-off (Fig. 7a and 7f). In essence, for light and heavy flow, traffic realigns without further amplification. For moderate traffic, we experience either a dipole or multiple cluster effect associated with start-and-go traffic flow.

6. Conclusion

The paper presents a new continuum second-order traffic flow equation that accounts for traffic viscosity on multi-lane highways. A new dynamic velocity equation was derived from the two-dimensional Navier-Stokes equation. The deduced equation was coupled with the classical LWR model to form the new viscous macroscopic model. The proposed model and its classical form are observed to have the same characteristic discriminant. The model was solved using an upwind finite difference scheme. This numerical scheme was implemented along with a Riemann initial condition and a Dirichlet boundary condition. Through the simulation results, it was realized that increasing the viscous rate will gradually cause the traffic to break down. A further simulation was carried out to determine the local effect of a minute perturbation on a homogeneous flow. We realized that the amplification of this displacement depends on the initial intensity of the traffic. The traffic blow-up within a certain neighborhood of the critical density.

References

[1] Lighthill, M.J., & Whitham, G.B. (1955). On kinematic waves II: A theory of traffic flow on long crowded roads. *Proceedings of the Royal Society of London. Series A Mathematical and Physical Sciences*, *229*(1178), 317-345.

[2] Richards, P.I. (1956). Shock waves on the highway. *Operations Research*, *4*(1), 42-51.

[3] Payne, H.J. (1971). *Models of freeway traffic and control.* In: G.A. Bekey (ed.), Mathematical Models of Public Systems (Simulation Council, La Jolla, CA), *1*, 51-61.

[4] Daganzo, C.F., Lin, W.H., & Del Castillo, J. (1997). A simple physical principle for the simulation of freeways with special lanes and priority vehicles. *Transportation Research Part B: Methodological*, *31*(2), 103-125.

[5] Lebacque, J.P. (2002). *A two phase extension of the LWR model based on the boundedness of traffic acceleration*. In: M. Taylor (ed.), Transportation and traffic theory in the 21st century. Proceedings of the 15th International Symposium on Transportation and Traffic Theory, p. 697-718.

[6] Whitham, G.B. (1974). *Linear and Nonlinear Waves*. New York: John Wiley and Sons.

[7] Daganzo, C.F. (1995). Requiem for second-order approximations of traffic flow. *Transportation Research B*, *29*(4), 277-286.

[8] Zhang, H.M. (1998). A theory of nonequilibrium traffic flow. *Transportation Research B*, *32*(7), 485-498.

[9] Zhang, H.M. (2002). A non-equilibrium traffic model devoid of gas-like behavior. *Transportation Research Part B*, *36*, 275-290.

[10] Aw, A., & Rascle, M. (2000). Resurrection of "second order" models of traffic flow. *SIAM Journal on Applied Mathematics*, *60*(3), 916-938.

[11] Jiang, R., Wu, Q.S., & Zhu, Z.J. (2002). A new continuum model for traffic flow and numerical tests. *Transportation Research Part B*, *36*, 405-419.

[12] Khan, Z.H., Gulliver, T.A., Nasir, H., Rehman, A., & Shahzada, K. (2019). A macroscopic traffic model based on physiological response. *Journal of Engineering Mathematics*, *115*(1), 21-41.

[13] Khan, Z.H., Imran, W., Azeem, S., Khattak, K.S., Gulliver, T.A., & Aslam M.S. (2019). A macroscopic traffic model based on driver reaction and traffic stimuli. *Applied Sciences*, *9*, 2848.

[14] Yu, L., Li, T., & Shi, Z. (2010). The effect of diffusion in a new viscous continuum traffic model. *Physics Letters A*, *374*, 2346-2355.

[15] Herty, M., Moutari, S., & Visconti, G. (2018). Macroscopic modeling of multi-lane motorways using a two-dimensional second-order model of traffic flow. *Society for Industrial and Applied Mathematics*, *78*(4), 2252-2278.

[16] Kühne, R. (1984). *Macroscopic freeway model for dense traffic-stop-start waves and incident detection.* In: J. Vollmuler & R. Hamerslag (ed). Proceedings of the 9th International Symposium on Transportation and Traffic Theory (ISTTT9), 21-42.

[17] Kerner, B.S., & Konhäuser, P. (1994). Structure and parameters of clusters in traffic flow. *Physical Review E*, *50*, 54-83.

[18] Berg, P., Mason, A., & Woods, A. (2000). Continuum approach to car-following models. *Physical Review E*, *61*, 1056-1066.

[19] Janna, W.S. (2010). *Introduction to Fluid Mechanics.* CRC Press, Taylor & Francis Group.

[20] Versteeg, H.K., & Malalasekera, W. (2007). *An Introduction to Computational Fluid Dynamics; The Finite Volume Method.* Pearson, Prentice Hall.

[21] Chandler, R., Herman, R., & Montroll, E. (1958). Traffic dynamics: Studies in car following. *Operations Research*, *6*(2), 165-184.

[22] Rosas-Jaimes, O.A., Luckie-Aguirre, O., & Rivera, J.C.L. (2013). Sensitivity parameter of a microscopic traffic model. *Congreso Nacional de Control Automático*, Ensenada, Baja California, Mexico.

[23] Del Castillo, J.M., & Benitez, F.G. (1995). On functional form of the speed-density relationship - i: general theory, ii: empirical investigation. *Transportation Research B*, *29*, 373-406.

[24] Courant, R., Friedrichs, K., & Lewy, H. (1967). On the partial difference equations of mathematical physics. *IBM Journal*, *11*, 215-234.

[25] British Columbia Ministry of Transportation (2003). Review and analysis of posted speed limits and speed limit setting practices in British Columbia.

[26] Herrmann, M., & Kerner, B.S. (1998). Local cluster effect in different traffic flow models. *Physica A*, *255*, 163-188.